HHS Public Access

Author manuscript

Anaerobe. Author manuscript; available in PMC 2020 October 01.

Published in final edited form as:

Anaerobe. 2019 October ; 59: 205–211. doi:10.1016/j.anaerobe.2019.102080.

Single cell analysis of nutrient regulation of *Clostridioides (Clostridium) difficile* motility

David S. Courson[1], **Astha Pokhrel**[1], **Cody Scott**[1], **Melissa Madrill**[1], **Alden J. Rinehold**[1], **Rita Tamayo**[2], **Richard E. Cheney**[3], **Erin B. Purcell**[1,✉]

[1]Department of Chemistry and Biochemistry, Old Dominion University, Norfolk, VA, USA

[2]Department of Microbiology and Immunology, University of North Carolina at Chapel Hill School of Medicine, Chapel Hill, NC, USA

[3]Department of Cell Biology and Physiology, Lineberger Comprehensive Cancer Center, University of North Carolina at Chapel Hill School of Medicine, Chapel Hill, NC US

Abstract

Regulation of bacterial motility to maximize nutrient acquisition or minimize exposure to harmful substances plays an important role in microbial proliferation and host colonization. The technical difficulties of performing high-resolution live microscopy on anaerobes have hindered mechanistic studies of motility in *Clostridioides (*formerly *Clostridium) difficile.* Here, we present a widely applicable protocol for live cell imaging of anaerobic bacteria that has allowed us to characterize *C. difficile* swimming at the single-cell level. This accessible method for anaerobic live cell microscopy enables inquiry into previously inaccessible aspects of *C. difficile* physiology and behavior. We present the first report that vegetative *C. difficile* are capable of regulated motility in the presence of different nutrients. We demonstrate that the epidemic *C. difficile* strain R20291 exhibits regulated motility in the presence of multiple nutrient sources by modulating its swimming velocity. This is a powerful illustration of the ability of single-cell studies to explain population-wide phenomena such as dispersal through the environment.

Keywords

Clostridioides (Clostridium) difficile; live cell anaerobic microscopy; motility regulation; nutrient regulation

Introduction

The gram-positive bacterium *Clostridioides* (formerly *Clostridium) difficile* was identified as a human pathogen in 1978 and classified by the Centers for Disease Control as an ‘urgent’

✉Corresponding Author Contact Information: Department of Chemistry and Biochemistry, Old Dominion University, 4541 Hampton Blvd, Norfolk, VA 23529, (757) 683-4240, epurcell@odu.edu.

public health threat in 2013[1,2]. *C. difficile* has become the most prevalent cause of hospital-acquired infections in the United States, and *C. difficile* infection (CDI) in the United States contributes to 46,000 deaths and $6B in economic costs annually[3–5]. In the past two decades, the emergence of epidemic strains associated with increased rates of CDI transmission, recurrence, and mortality has compounded the public health threat presented by *C. difficile*[5–11]. CDI is spread between patients by spores, *C. difficile* cells that have differentiated into a metabolically dormant, highly resilient form that is impervious to chemical disinfectants and ethanol-based sanitizers[12]. Due to the fact that *C. difficile* is an obligate anaerobe in its metabolically active, or vegetative, form, microscopic information about microbial behavior is limited[13,14].

Most *C. difficile* strains produce flagella and are motile, capable of swimming through liquid or semi-solid media[15]. *C. difficile* is also capable of flagellum-independent movement upon solid surfaces via the extension and retraction of Type IV pili[16]. Disruption of either flagellum or pilus genes reduces the ability of *C. difficile* to colonize animal hosts [17,18] Motility assays measuring the ability of *C. difficile* strains to swim through soft agar medium have shown that the epidemic-associated, ribotype 027 strain R20291 disperses via motility more quickly than the historical 630Δ*erm* strain, but it is not known whether this plays a role in the observed higher virulence of R20291 within mammalian hosts [6,11,15,19].

Many motile bacteria can regulate their motility in response to extracellular signals by regulating the activity of the motor complexes that rotate their flagella [20,21]. Sustained periods of flagellar rotation result in unidirectional ‘runs’ by the cell, while transient changes in rotational direction or speed result in ‘tumbles’ that randomly reorient bacterial cells to run in new directions[22–29]. Long runs result in bacterial dispersal, while frequent tumbles shorten run length and geographically constrain the cells[22,26]. The speed of flagellar rotation can also affect bacterial dispersal, as slower rotation results in less displacement[23,27,30]. Bacteria can alter their tumbling frequency and/or their velocity to bias their motility towards a more concentrated source of nutrients or other chemoattractant, or to limit their exposure to toxic or growth-inhibiting substances such as phenols or alcohols[20,30]. In many intestinal pathogens, including *Helicobacter pylori, Salmonella* Typhimurium, and *Vibrio cholerae,* directional motility to or through the mucus layer that coats the intestinal epithelium is necessary for full virulence[31–38].

C. difficile is highly responsive to nutrient availability in its environment. Toxin production *in vitro* is repressed or stimulated by the nutrient content of the growth medium, and disease severity within animal hosts may be affected by host dietary restriction[39–43]. The protection against *C. difficile* infection provided by a robust community of commensal gut bacteria depends at least partially on those bacteria metabolizing the available nutrients in the large intestine so efficiently that *C. difficile* cannot establish colonization[44–46]. Disruption of the gut microbiota by antibiotic treatments, the major clinical risk factor for CDI, causes a transient increase in nutrient availability as the gut bacterial ecosystem is perturbed, creating a metabolic niche for *C. difficile*[47–49]. *C. difficile* readily metabolizes monosaccharides, which are not highly prevalent in mammalian large intestines unless the native gut microbiota have been disrupted by prior antibiotic exposure[45,48,50]. In an *in vitro* model of this nutrient-based colonization resistance, mouse intestinal flora inoculated into growth

medium made from the cecal contents of gnotobiotic mice deplete the carbohydrates and amino acids enough to prevent *C. difficile* replication[44]. Supplementation with the monosaccharides glucose, N-acetylglucosamine (GlcNAc), or N-acetylneuraminic acid (Neu5A) is sufficient to overcome this microbiota-dependent starvation and enable *C. difficile* cell division[44]. Both GlcNAc and Neu5A are components of intestinal mucus, and both serve as chemoattractants for the intestinal pathogen *Vibrio cholerae*[51]. Concentrations of Neu5A in the murine gut increase after treatment with antibiotics, suggesting that Neu5A contributes to favorable conditions for *C. difficile* colonization[48].

Nutrient availability is a signal that regulates *C. difficile* gene transcription, spore formation, and metabolism of the second messenger molecule cyclic diguanylate, but nutrient regulation of motility has not previously been reported in this organism[39–41,52,53]. In this work, we present a technique that can be used to image anaerobic bacteria outside of an anaerobic chamber on nearly any inverted microscope. Obligate anaerobes can grow and survive in the imaging chamber for extended periods without succumbing to oxygen toxicity. We used this system to perform single-cell motility assays and demonstrate for the first time that *C. difficile* regulates its motility in the presence N-acetylneuraminic acid, a metabolite linked to *C. difficile* colonization *in vivo.* We report that this organism controls its motility in response to environmental cues by altering its swimming velocity during unidirectional runs rather than by modulating its tumble frequency. The ability to perform extended live cell microscopy on *C. difficile* on a standard microscope with no specialized attachments will provide new insights into vegetative *C. difficile* physiology and behavior and contribute to a more complete understanding of the stage of the *C. difficile* life cycle.

Materials and Methods

Bacterial strains and growth conditions

C. difficile strain R20291 was grown in brain heart infusion medium supplemented with yeast extract (5 g/L) (BHIS)[54] in an anaerobic chamber at 37°C with an atmosphere of 85% N_2, 10% CO_2, 5% H_2. Migration assays were performed in BHIS and BHIS with 0.3% agar supplemented with glucose, arabinose, or N-acetylneuraminic acid (Fisher Scientific) at the indicated concentrations. Growth curves were performed in BHIS supplemented with the indicated saccharides to a final concentration of 32 mM, inoculated 1:20 with saturated overnight culture of *C. difficile* R20291. Doubling times were calculated in Prism (GraphPad) software using non-linear curve fits to the exponential growth equation $Y = Y_0 * \exp(k*X)$ where Y_0 is the initial optical density, Y is the measured optical density, and X is time. Doubling times were determined by fitting the data between 0 and 5 hours to exclude rollover into stationary phase.

Macroscopic motility assays

Migration assays were carried out in supplemented or unsupplemented BHIS with 0.3% agar. Arabinose, glucose, or N-acetylneuraminic acid was added to molten medium to the indicated final concentration. Plates were poured and allowed to solidify on the laboratory bench overnight, then transferred to the anaerobic chamber to equilibrate for 24 hours before use. Sterilized toothpicks were used for inoculation of individual colonies of R20291 into

the agar medium. Each toothpick was used to stab the soft agar plate twice to allow for duplicate measurements. Migration diameters were measured after 12 and 24 hours of incubation at 37°C. The mean diameters and standard deviations of the motility measurements of four biologically independent samples measured in duplicate are reported. One biological replicate was excluded from the 24 hour BHIS condition because the populations grew into each other and could not be measured separately. Migration in supplemented and unsupplemented BHIS at each time point was compared using two-way analysis of variance with Tukey's multiple-comparison post-test.

Imaging chamber construction

Sealed rose chambers with gas impermeable gaskets were constructed to allow long-term imaging of anaerobic bacteria with an aerobic microscope as detailed in ([55]). Aluminum top and bottom plates with imaging windows were machined for use with a Nikon Ti-E inverted microscope and 25 mm square glass coverslips. Screw holes were milled into each corner. Gaskets were cut from 3 mm thick rubber with a central opening 18 mm in diameter and screw holes aligned to those in the aluminum chamber plates. Before use, all components were sterilized by soaking in 10% bleach for at least 60 minutes, rinsed in deionized water, and allowed to dry completely. The assembled imaging chamber holds a sample volume of approximately 800 μL and has internal surfaces of biologically inert glass and rubber.

Imaging chamber assembly

Rose chambers were assembled and screwed shut at the laboratory bench. Gaskets were placed between two glass coverslips and the resulting 'sandwich' was placed between the aluminum plates and sealed with screws. To inject materials into the chamber, 25 gauge (0.5 mm) needles were inserted through opposite faces of the gasket with needle tips extending into the central opening. Chambers were taken into the anaerobic chamber with needles still inserted through the rubber gasket and allowed to equilibrate for 24 hours unless otherwise indicated in order to allow complete off-gassing of molecular oxygen.

Sample preparation for imaging

Starter cultures of *C. difficile* R20291 were grown overnight in BHIS medium. These cultures were diluted 1:50 and allowed to grow for three hours. The diluted culture (150 μL) was then mixed with 1.35 mL of fresh BHIS supplemented with the indicated concentration of N-acetylneuraminic acid. The sample was loaded into a syringe, then, holding the chamber vertically, the sample was injected through the bottom port of the chamber, until all gas escaped through the top needle. Both needles were removed, allowing the holes in the rubber gasket to reseal. The edges of the sealed imaging chamber were then wrapped in parafilm and removed from the anaerobic chamber, and the exterior of the chamber was sterilized with 10% bleach and 70% ethanol before imaging to prevent contamination of workspaces. Each chamber was transported to the microscope for imaging immediately upon assembling; microscopy began roughly 8 minutes after chamber assembly.

Microscopy

Live-cell, time-lapse differential interference contrast (DIC) microscopy was performed on a Nikon Ti-E inverted microscope equipped with Nikon Perfect Focus System, apochromat TIRF 60X Oil Immersion Objective Lens (numerical aperture 1.49), a condenser (numerical aperture 0.52), pco.edge 4.2 LT sCMOS camera, and SOLA SE II 365 Light Engine as well as complementary DIC components. Stage temperature was maintained at 36.5°C +/− 0.5°C using a Nevtek Air Stream microscope stage warmer and home-built microscope enclosure. Movies were recorded using 100 ms exposures at a frame rate of 10 frame/s for 10 seconds. Three movies at independent, randomly selected locations were recorded for each sample. At least three biologically independent samples were imaged in each medium condition. The first ten cells to enter each viewing field were analyzed, resulting in 84–90 cells analyzed per medium condition. Data shown are means and standard deviations of all cells analyzed in a given condition.

Imaging chamber decontamination

When imaging was completed, the microscope stage and sample holder were wiped down with 10% bleach and 70% ethanol. The parafilm wrap was placed into biohazard waste and the intact sample chamber was submerged in a 50% bleach solution. The chamber was disassembled while submerged and all the components were allowed to soak for 10 minutes. Coverslips were removed and discarded as biohazardous waste. Aluminum and rubber components were rinsed with deionized water and then soaked in 117 mM sodium thiosulfate for 30 minutes to neutralize any residual bleach. Components were then washed with ethanol and dried before being used again. Rubber gaskets were discarded after 3 uses (6 piercings) or if the coverslip did not easily dissociate during the bleach soak. Metal hardware can be reused indefinitely, if properly cared for.

Data Analysis

Image analysis was performed using Fiji/ImageJ[56]. The line segment tool was used to measure unidirectional displacement of each bacterial cell over time. Each reorientation was considered the culmination of a run and the start of a new run. The movement of at least ten cells was documented during each movie. The run lengths, run durations, and number of tumbles were recorded for each cell. For run length analysis, only runs whose beginnings and ends occurred within the field of view and plane of focus were considered. Swimming velocity was calculated by dividing individual run lengths by the elapsed time of the run. Net displacement of a cell was calculated by measuring the distance between a given cells starting and ending position over the length of the observation window. Displacement, run length, cellular velocity, and tumbling frequency at each of the indicated concentrations of N-acetylneuraminic acid were compared by one-way analysis of variance using Tukey’s multiple comparison test. Statistical analysis was performed using Prism (GraphPad version 6.0c).

Results and Discussion

Clostridioides difficile exhibits regulated motility in the presence of nutrients

Regulated motility allows bacteria to preferentially travel towards areas of greater attractant concentration. If nutrients or other attractants are uniformly present throughout a bacterial growth medium, their presence will suppress bacterial swimming away from the site of inoculation, as cells will be less 'motivated' to seek additional nutrient sources[57]. The *C. difficile* genome contains a single predicted methyl-accepting chemotaxis protein (CDR20291_0463) within a putative chemotaxis operon (CDR20291_0458 to CDR20291_0467), suggesting that *C. difficile* may regulate its flagellar motility in response to nutrients. As N-acetylneuraminic acid (Neu5A) is positively associated with *C. difficile* growth in animal models [44,48], we tested its effect on *C. difficile* motility to determine whether Neu5A affects the motility of this organism. We similarly tested the effect of medium supplementation with glucose. To control for the possibility that Neu5A and glucose were changing the osmolarity of the medium in addition to serving as nutrient sources, we also tested the effect of supplementation with arabinose, which *C. difficile* cannot metabolize[58]. When individual colonies of *C. difficile* R20291 were inoculated into BHIS medium with 0.3% agar, which has a viscosity similar to that of intestinal mucus[59–61], cells spread symmetrically through the agar. Medium supplementation with 1% of any carbohydrate reduced motility after 12 hours, with 1% glucose reducing migration by 33% and 1% Neu5A reducing migration 85% (Figure 1A). Supplementation with arabinose reduced motility 18% after 12 hours, indicating that addition of additional solutes to a growth medium can suppress motility slightly even when those solutes are not metabolically available for catabolism (Figure 1A). After 24 hours of migration through 0.3% agar, supplementation with arabinose has no significant effect on migration diameter, suggesting that *C. difficile* has successfully adapted to the nutrient-independent effects of medium supplementation. Supplementation with 1% glucose reduces 24 hour migration from the inoculation site by 22%, and supplementation with 1% Neu5A reduces it by 69%, indicating the presence of metabolically accessible nutrients inhibits *C. difficile* dispersal through the environment (Figure 1B,F). To ensure that the observed motility differences upon supplementation with 1% saccharide were not due to discrepant molar concentrations of the supplements, we repeated these motility assays with 32 mM arabinose and glucose, the molar concentration of 1% Neu5A. We found that neither arabinose nor glucose at 32 mM had any significant effect on motility through soft agar (Figure 1 C, D). None of the indicated sugars slowed growth in liquid culture at 32 mM, confirming that the observed effects of nutrient supplementation in soft agar are due to inhibition of motility rather than a reduction in cell replication (Figure 1E, Figure S1, Table 1). These results are consistent with *C. difficile* sensing local nutrient availability and reducing its motility away from locations in which nutrients are abundant.

Rose chambers allow long-term imaging of live C. difficile on a standard inverted microscope

To conduct microscopic analysis of *C. difficile* motility on a standard inverted microscope, we utilized a rose chamber. This approach involves assembling metal plates to sandwich a rubber gasket with a central hole between two coverslips to create a self-contained imaging

chamber (Figure 2A)[55,62]. The rubber gasket can be pierced with a standard needle, allowing gas and fluid exchange with the surrounding environment. Placement of a second needle vents displaced air, allowing sample injection into an assembled chamber (Figure 2B). Importantly, the gasket seals itself upon removal of the needles. Assembled chambers can be equilibrated in the anaerobic chamber and injected with a sample of cells in desired media. When needles are removed the bacteria are sealed inside a portable anaerobic environment. The chamber was placed on the microscope and maintained at 37°C. Within this device, *C. difficile* cells exhibited cell growth and division for extended periods. Images were recorded at various time points while the cells grew. After 6 hours within the rose chamber, bacteria were visually confirmed to continue swimming and increase in cell density, confirming that the rose chambers maintain *C. difficile* viability during this timeframe (Figure 2C).

Single-cell analysis of C. difficile motility

In order to measure motility in different media, rather than cell growth, we recorded fast time-lapse videos immediately following chamber assembly. Recordings were completed within 15 minutes of chamber assembly. To prepare culture for imaging a saturated overnight culture was diluted 1:50 into fresh media and allowed to acclimate for three hours, comparable to the lag phase *C. difficile* cells exhibit between inoculation into fresh media and the onset of exponential growth (Figure 1E). Chambers were filled with 1:10 dilutions of exponential culture.

To quantify bacterial motility within the rose chamber, we measured net displacement, unidirectional run length, velocity during unidirectional runs, and tumble frequency of at least ten randomly selected cells within each movie. Velocity during unidirectional run and net displacement during the 10 second runs were also measured; as some cells tumbled to change direction one or more times, net displacement was sometimes less than total distance travelled. In BHIS medium, individual *C. difficile* R20291 cells traveled with an average velocity of 21.3 μm/s and exhibited an average net displacement of 88.4 μm over the course of 10 seconds (Movie 1) (Figure 3). The majority of the cells analyzed (53.4%), exhibited no tumbling within 10 second analysis windows; of the subset that did tumble, the average tumbling frequency was 0.32/s (Figure 4).

To determine whether the suppressive effect of Neu5A on *C. difficile* motility observed in entire populations (Figure 1) could be detected in single cells, we quantified motility of individual cells through medium supplemented with 10 mM, 16 mM, 25 mM, and 32 mM (corresponding to 1%) N-acetylneuraminic acid. Supplementation with 10 mM Neu5A had no significant effect on net displacement, while 16 mM Neu5A caused a small but significant increase in displacement. Increasing concentrations of Neu5A had an inhibitory effect on displacement. Supplementation with 25 mM Neu5A reduced net displacement 20% from 88.4 μm to 71.0 μm, and 50 mM Neu5A further reduced displacement 78% to 19.1 μm (Figure 3A). This reduction in single-cell motility is consistent with the lower-resolution migration analysis performed on agar plates (Figure 1), validating the microscopic approach.

To determine whether the reduction in cellular displacement in the presence of Neu5A is due to reduced swimming speeds, we quantified the velocities of individual cells. As time spent reorienting during a tumble decreases net displacement during a given period of motility, we

measured run velocity only during unidirectional runs (defined as three or more consecutive frames of movement in the same direction) and excluded frames in which cells were altering the direction of their movements. By quantifying run velocity in this way, we observed that supplementation with Neu5A reduced swimming velocity in a dose-dependent manner. 10 mM and 16 mM Neu5A had no significant effect on swimming velocity, but supplementation with 25 mM Neu5A reduces velocity 26%, from 21.3 μm/s to 15.8 μm/s, and supplementation with 50 mM Neu5A nearly halted motility, reducing velocity 75% to 5.4 μm/s (Videos 2–5) (Figure 3B).

Reduced swimming velocity is not the only mechanism by which bacterial cells can limit their dispersal away from nutrients. Many bacteria stay ‘in place’ through increased tumbling, shortening their unidirectional run length. To determine whether *C. difficile* alters its tumble frequency as well as its run velocity, we quantified the reorientations of individual cells (see Video 1, 8.5 seconds for an example). Because not all of the cells analyzed remained in-frame for the full ten seconds of recording, we reported the number of tumbles per second of recorded motility. We found that the average tumble frequency was not significantly affected by supplementation with any concentration of Neu5A (Figure 4A). The majority of the cells observed did not tumble during 10 second observation windows, and nutrient supplementation did not have any appreciable effect on this (Figure 4B). Of the subset of cells that did tumble, the addition of Neu5A actually appeared to decrease tumble frequency. The majority of the tumbling cells in all medium conditions tumbled 0.1–0.25 times/sec. Only 7.3% of cells incubated in 32 mM Neu5A tumbled more than 0.25 times/s, compared to 10–20% of the cells in other media conditions, and none exceeded 0.5 tumbles/s, compared to 4–10% of the cells in other conditions (Figure 4B). The average reorientation frequency of tumbling cells in 1% Neu5A was 0.22 tumbles/s, lower than 0.32 tumbles/sec in unsupplemented BHIS or in any of the lower Neu5A concentrations (Figure 4C). While these differences were not statistically significant, they do demonstrate that *C. difficile* sensing of Neu5A does not increase tumbling frequency and rules this out as a mechanism for Neu5A-dependent reduction of motility.

Conclusions

It is clear that *C. difficile* suppresses its motile dispersal through the environment when in nutritionally favorable conditions. When added to semisolid growth medium at 1%, both Neu5A and glucose are capable of reducing *C. difficile* motility at the population level, while the non-metabolizable saccharide arabinose has no sustained effect over 24 hours. The molar concentration needed to reduce motility is higher for glucose (55 mM at 1 %) than for Neu5A (32 mM at 1%). As Neu5A supplies nitrogen as well as carbon, it is unclear whether its more potent effect on motility is specific or is a more general read-out of the bacterium’s global metabolic state. This organism does encode predicted chemotaxis genes, so it is possible that this regulation contributes to directional motility in the presence of gradients. More extensive future studies could identify potential nutritional regulators of *C. difficile* motility and the role of its putative chemoreceptor.

Single cell motility analysis on a microscope and population-level migration assays on agar plates lead to the same conclusion—that the infection-associated nutrient Neu5A suppresses

C. difficile motility. However, the microscopy method yields the additional information that the observed decrease in *C. difficile* dispersal observed in the presence of Neu5A can be attributed entirely to a decrease in swimming velocity and not to any increase in tumbling frequency. Indeed, cellular displacement decreases despite a slight observed decrease in tumbling frequency. The microscopy method also uses significantly smaller quantities of reagent. This study illustrates the utility of live microscopy and single cell analysis in investigating bacterial behavioral phenotypes. The use of rose chambers to image anaerobic bacteria on a standard inverted microscope allows the rapid collection of mechanistic data that were previously very difficult to access. In the future, this technique will allow assessment of *C. difficile* responses to other nutrient sources, to environmental stresses, and even to mammalian cells, providing novel insights into the physiology and behavior of vegetative *C. difficile.*

Supplementary Material

Refer to Web version on PubMed Central for supplementary material.

Acknowledgements

The authors declare no financial conflicts of interest. This work was funded by NIAID 1K22AI118929–01. EBP was supported by a Summer Research Fellowship Program Grant from the Office of Research at Old Dominion University, Norfolk, Virginia, USA. CS and MM were supported by a Program for Undergraduate Research and Scholarship award from the Office of Research at Old Dominion University, Norfolk, Virginia, USA. RT was supported by NIAID R01AI107029.

Works Cited

1. Larson HE, Price AB, Honour P & Borriello SP Clostridium difficile and the aetiology of pseudomembranous colitis. Lancet. 1 (8073), 1063–1066, (1978). [PubMed: 77366]
2. Services, U. S. D. o. H. a. H. (Centers for Disease Control and Prevention, US Department of Health and Human Services, Atlanta, GA, 2013).
3. Services, U. S. D. o. H. a. H. Nearly half a million Americans suffered from Clostridium difficile infections in a single year, <https://http://www.cdc.gov/media/releases/2015/p0225-clostridium-difficile.html> (2015).
4. Shorr AF, Zilberberg MD, Wang L, Baser O & Yu H Mortality and Costs in Clostridium difficile Infection Among the Elderly in the United States. Infect Control Hosp Epidemiol. 37 (11), 1331–1336, (2016). [PubMed: 27572289]
5. See I et al. NAP1 strain type predicts outcomes from Clostridium difficile infection. Clin Infect Dis. 58 (10), 1394–1400, (2014). [PubMed: 24604900]
6. Denève C, Janoir C, Poilane I, Fantinato C & Collignon A New trends in Clostridium difficile virulence and pathogenesis. International Journal of Antimicrobial Agents. 33 S24–S28. [PubMed: 19303565]
7. Stabler RA et al. Comparative genome and phenotypic analysis of Clostridium difficile 027 strains provides insight into the evolution of a hypervirulent bacterium. Genome Biol. 10 (9), R102, (2009). [PubMed: 19781061]
8. Merrigan M et al. Human Hypervirulent Clostridium difficile Strains Exhibit Increased Sporulation as Well as Robust Toxin Production. Journal of Bacteriology. 192 (19), 4904–4911, (2010). [PubMed: 20675495]
9. Bartlett JG Clostridium difficile: progress and challenges. Ann N Y Acad Sci. 1213 62–69, (2010). [PubMed: 21175676]

10. Valiente E, Dawson LF, Cairns MD, Stabler RA & Wren BW Emergence of new PCR ribotypes from the hypervirulent Clostridium difficile 027 lineage. J Med Microbiol. 61 (Pt 1), 49–56, (2012). [PubMed: 21903827]
11. Smits WK Hype or hypervirulence: a reflection on problematic C. difficile strains. Virulence. 4 (7), 592–596, (2013). [PubMed: 24060961]
12. Rodriguez-Palacios A & Lejeune JT Moist-heat resistance, spore aging, and superdormancy in Clostridium difficile. Appl Environ Microbiol. 77 (9), 3085–3091, (2011). [PubMed: 21398481]
13. Holy O & Chmelaf D Oxygen tolerance in anaerobic pathogenic bacteria. Folia Microbiologica. 57 (5), 443–446, (2012). [PubMed: 22573259]
14. Edwards AN et al. Chemical and Stress Resistances of Clostridium difficile Spores and Vegetative Cells. Front Microbiol. 7 1698, (2016). [PubMed: 27833595]
15. Purcell EB, McKee RW, McBride SM, Waters CM & Tamayo R Cyclic Diguanylate Inversely Regulates Motility and Aggregation in Clostridium difficile. Journal of Bacteriology. 194 (13), 3307–3316, (2012). [PubMed: 22522894]
16. Purcell EB, McKee RW, Bordeleau E, Burrus V & Tamayo R Regulation of Type IV Pili Contributes to Surface Behaviors of Historical and Epidemic Strains of Clostridium difficile. J Bacteriol. 198 (3), 565–577, (2015). [PubMed: 26598364]
17. Batah J et al. Clostridium difficile flagella induce a pro-inflammatory response in intestinal epithelium of mice in cooperation with toxins. Sci Rep. 7 (1), 3256–3256, (2017). [PubMed: 28607468]
18. McKee RW, Aleksanyan N, Garrett EM & Tamayo R Type IV Pili Promote Clostridium difficile Adherence and Persistence in a Mouse Model of Infection. Infect Immun. 86 (5), (2018).
19. Loo VG et al. A predominantly clonal multi-institutional outbreak of Clostridium difficile-associated diarrhea with high morbidity and mortality. N Engl J Med. 353 (23), 2442–2449, (2005). [PubMed: 16322602]
20. Eisenbach M Control of bacterial chemotaxis. Mol Microbiol. 20 (5), 903–910, (1996). [PubMed: 8809743]
21. Roberts MA, Papachristodoulou A & Armitage JP Adaptation and control circuits in bacterial chemotaxis. Biochem Soc Trans. 38 (5), 1265–1269, (2010). [PubMed: 20863296]
22. Berg HC & Brown DA Chemotaxis in Escherichia coli analysed by three-dimensional tracking. Nature. 239 (5374), 500–504, (1972). [PubMed: 4563019]
23. Macnab RM & Koshland DE The Gradient-Sensing Mechanism in Bacterial Chemotaxis. Proc Natl Acad Sci US A. 69 (9), 2509–2512, (1972).
24. Larsen SH, Reader RW, Kort EN, Tso WW & Adler J Change in direction of flagellar rotation is the basis of the chemotactic response in Escherichia coli. Nature. 249 (452), 74–77, (1974). [PubMed: 4598031]
25. Armitage JP & Macnab RM Unidirectional, intermittent rotation of the flagellum of Rhodobacter sphaeroides. J Bacteriol. 169 (2), 514–518, (1987). [PubMed: 3492489]
26. Turner L, Ryu WS & Berg HC Real-time imaging of fluorescent flagellar filaments. J Bacteriol. 182 (10), 2793–2801, (2000). [PubMed: 10781548]
27. Eisenbach M in eLS 10.1002/9780470015902.a0001251.pub3 (John Wiley & Sons, Ltd, 2011).
28. Garrity LF & Ordal GW Chemotaxis in Bacillus subtilis: How bacteria monitor environmental signals. Pharmacology & Therapeutics. 68 (1), 87–104, (1995). [PubMed: 8604438]
29. Rao CV, Glekas GD & Ordal GW The three adaptation systems of *Bacillus subtilis* chemotaxis. Trends Microbiol. 16 (10), 480–487, (2008). [PubMed: 18774298]
30. Porter SL, Wadhams GH & Armitage JP Signal processing in complex chemotaxis pathways. Nat Rev Microbiol. 9 (3), 153–165, (2011). [PubMed: 21283116]
31. Pittman MS, Goodwin M & Kelly DJ Chemotaxis in the human gastric pathogen Helicobacter pylori: different roles for CheW and the three CheV paralogues, and evidence for CheV2 phosphorylation. Microbiology. 147 (Pt 9), 2493–2504, (2001). [PubMed: 11535789]
32. Croxen MA, Sisson G, Melano R & Hoffman PS The Helicobacter pylori chemotaxis receptor TlpB (HP0103) is required for pH taxis and for colonization of the gastric mucosa. J Bacteriol. 188 (7), 2656–2665, (2006). [PubMed: 16547053]

33. Huang JY et al. Chemodetection and Destruction of Host Urea Allows Helicobacter pylori to Locate the Epithelium. Cell Host Microbe. 18 (2), 147–156, (2015). [PubMed: 26269952]
34. Stecher B et al. Flagella and chemotaxis are required for efficient induction of Salmonella enterica serovar Typhimurium colitis in streptomycin-pretreated mice. Infect Immun. 72 (7), 4138–4150, (2004). [PubMed: 15213159]
35. Freter R, O'Brien PC & Macsai MS Role of chemotaxis in the association of motile bacteria with intestinal mucosa: in vivo studies. Infect Immun. 34 (1), 234–240, (1981). [PubMed: 7298185]
36. Bordas MA, Balebona MC, Rodriguez-Maroto JM, Borrego JJ & Morinigo MA Chemotaxis of pathogenic Vibrio strains towards mucus surfaces of gilt-head sea bream (Sparus aurata L.). Appl Environ Microbiol. 64 (4), 1573–1575, (1998). [PubMed: 9575135]
37. O'Toole R et al. The chemotactic response of Vibrio anguillarum to fish intestinal mucus is mediated by a combination of multiple mucus components. J Bacteriol. 181 (14), 4308–4317, (1999). [PubMed: 10400589]
38. Larsen MH, Larsen JL & Olsen JE Chemotaxis of Vibrio anguillarum to fish mucus: role of the origin of the fish mucus, the fish species and the serogroup of the pathogen. FEMS Microbiology Ecology. 38 (1), 77–80, (2001).
39. Antunes A, Martin-Verstraete I & Dupuy B CcpA-mediated repression of Clostridium difficile toxin gene expression. Mol Microbiol. 79 (4), 882–899, (2011). [PubMed: 21299645]
40. Dineen SS, McBride SM & Sonenshein AL Integration of metabolism and virulence by Clostridium difficile CodY. J Bacteriol. 192 (20), 5350–5362, (2010). [PubMed: 20709897]
41. Karlsson S, Burman LG & Akerlund T Suppression of toxin production in Clostridium difficile VPI 10463 by amino acids. Microbiology. 145 (7), 1683–1693, (1999). [PubMed: 10439407]
42. Blankenship-Paris TL, Chang J, Dalldorf FG & Gilligan PH In vivo and in vitro studies of Clostridium difficile-induced disease in hamsters fed an atherogenic, high-fat diet. Lab Anim Sci. 45 (1), 47–53, (1995). [PubMed: 7752614]
43. Mahe S, Corthier G & Dubos F Effect of various diets on toxin production by two strains of Clostridium difficile in gnotobiotic mice. Infect Immun. 55 (8), 1801–1805, (1987). [PubMed: 3610315]
44. Wilson KH & Perini F Role of competition for nutrients in suppression of Clostridium difficile by the colonic microflora. Infect Immun. 56 (10), 2610–2614, (1988). [PubMed: 3417352]
45. Nguyen D et al. Active starvation responses mediate antibiotic tolerance in biofilms and nutrient-limited bacteria. Science. 334 (6058), 982–986, (2011). [PubMed: 22096200]
46. Hooper LV, Midtvedt T & Gordon JI How Host-Microbial Interactions Shape the Nutrient Environment of the Mammalian Intestine. Annual Review of Nutrition. 22 (1), 283–307, (2002).
47. Ng KM et al. Microbiota-liberated host sugars facilitate post-antibiotic expansion of enteric pathogens. Nature. 502 (7469), 96–99, (2013). [PubMed: 23995682]
48. Theriot CM et al. Antibiotic-induced shifts in the mouse gut microbiome and metabolome increase susceptibility to Clostridium difficile infection. Nat Commun. 5 3114, (2014). [PubMed: 24445449]
49. Fletcher JR, Erwin S, Lanzas C & Theriot CM Shifts in the Gut Metabolome and Clostridium difficile Transcriptome throughout Colonization and Infection in a Mouse Model. mSphere. 3 (2), e00089–00018, (2018). [PubMed: 29600278]
50. Jenior ML, Leslie JL, Young VB & Schloss PD Clostridium difficile Colonizes Alternative Nutrient Niches during Infection across Distinct Murine Gut Microbiomes. mSystems. 2 (4), (2017).
51. Reddi G, Pruss K, Cottingham KL, Taylor RK & Almagro-Moreno S Catabolism of mucus components influences motility of Vibrio cholerae in the presence of environmental reservoirs. PLoS One. 13 (7), e0201383, (2018). [PubMed: 30048543]
52. Edwards AN, Nawrocki KL & McBride SM Conserved Oligopeptide Permeases Modulate Sporulation Initiation in Clostridium difficile. Infect Immun. 82 (10), 4276–4291, (2014). [PubMed: 25069979]
53. Purcell EB et al. A nutrient-regulated cyclic diguanylate phosphodiesterase controls Clostridium difficile biofilm and toxin production during stationary phase. Infect Immun. 10.1128/iai. 00347-17, (2017).

54. Smith CJ, Markowitz SM & Macrina FL Transferable tetracycline resistance in Clostridium difficile. Antimicrob Agents Chemother. 19 (6), 997–1003, (1981). [PubMed: 7271279]

55. Wadsworth P Studying Mitosis in Cultured Mammalian Cells. Cold Spring Harbor Protocols. 2007 (2), pdb.prot4674, (2007).

56. Schindelin J et al. Fiji: an open-source platform for biological-image analysis. Nat Methods. 9 676, (2012). [PubMed: 22743772]

57. Adler J Chemotaxis in bacteria. Science. 153 (3737), 708–716, (1966). [PubMed: 4957395]

58. Nakamura S, Nakashio S, Yamakawa K, Tanabe N & Nishida S Carbohydrate Fermentation by Clostridium difficile. Microbiol Immunol. 26 (2), 107–111, (1982). [PubMed: 6806571]

59. Swidsinski A et al. Viscosity gradient within the mucus layer determines the mucosal barrier function and the spatial organization of the intestinal microbiota. Inflamm Bowel Dis. 13 (8), 963–970, (2007). [PubMed: 17455202]

60. Fan Y et al. Novel amelogenin-releasing hydrogel for remineralization of enamel artificial caries. Journal of bioactive and compatible polymers. 27 (6), 585–603, (2012). [PubMed: 23338820]

61. Lai SK, Wang Y-Y, Wirtz D & Hanes J Micro- and macrorheology of mucus. Advanced drug delivery reviews. 61 (2), 86–100, (2009). [PubMed: 19166889]

62. de Jong IG, Beilharz K, Kuipers OP & Veening J-W Live Cell Imaging of Bacillus subtilis and Streptococcus pneumoniae using Automated Time-lapse Microscopy. J Vis Exp. 10.3791/3145 (53), 3145, (2011). [PubMed: 21841760]

Highlights

- Live anaerobic bacteria can be imaged on a standard microscope.
- *Clostridium difficile* modulates its swimming velocity in response to nutrient availability.
- The gastric mucus component N-acetylneuraminic acid regulates *C. difficile* motility.

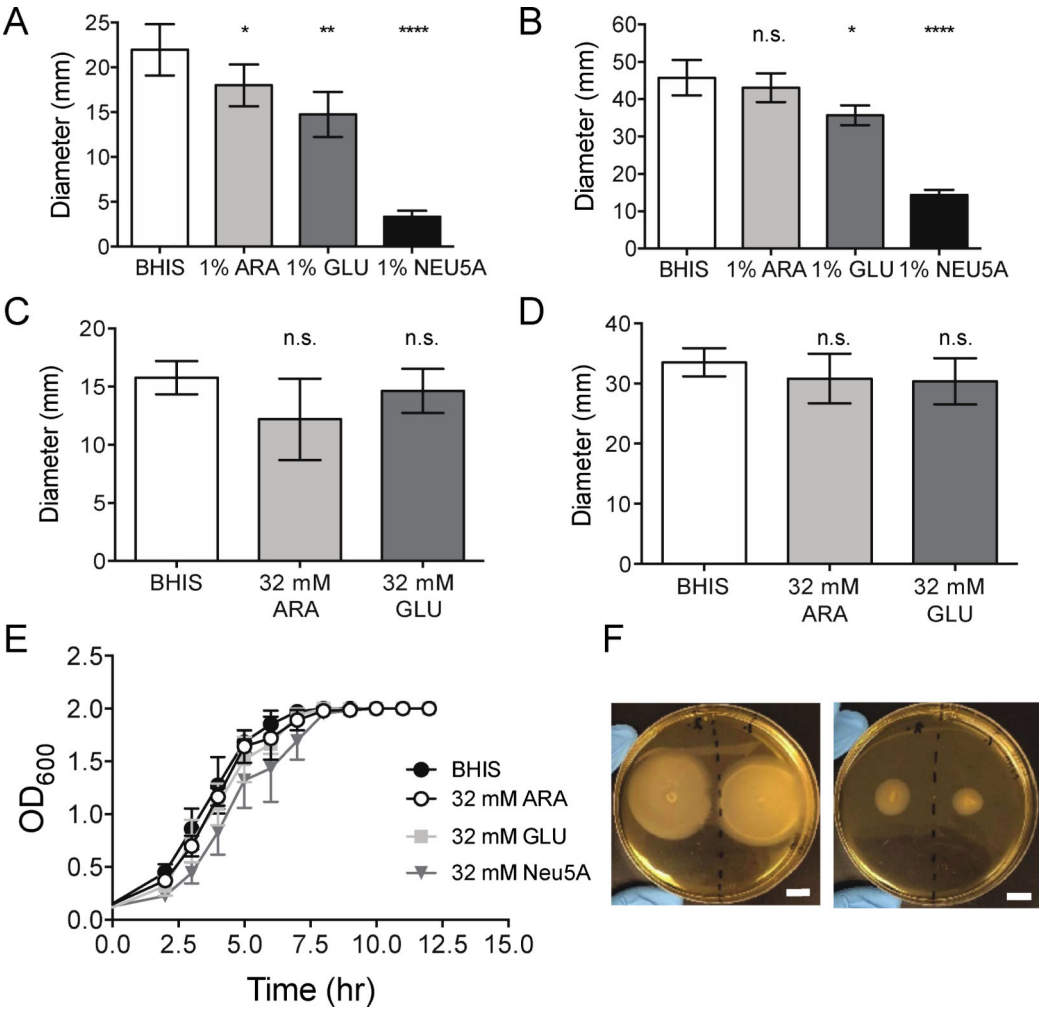

Figure 1. *C. difficile* motility through soft agar is constrained by nutrients.

(A,B) Migration of *C. difficile* R20291 through semi-solid BHIS supplemented with 1% arabinose (ARA), glucose (GLU), or N-acetylneuraminic acid (Neu5A). (C,D) Migration of *C. difficile* R20291 through semi-slid BHIS supplemented with 32 mM arabinose (ARA) or glucose (GLU), equimolar to 1% Neu5A. Motility diameters were measured 12 (A,C) or 24 (B,D) hours after inoculation by stabbing. Measurements represent the means and standard deviations of four biologically independent swarms per condition, measured in duplicate. Motility in each supplemented medium was compared to motility in BHIS-agar by unpaired t-test; n.s. not significant, * $p < 0.05$, ** $p < 0.01$ **** $p < 0.0001$. (E) Growth of *C. difficile* R20291 in liquid BHIS with or without supplementation with 32 mM of the indicated saccharides. (F) Representative images of *C. difficile* R20291 24 hours after inoculation into BHIS 0.3% agar in the presence (left) or absence (right) of 1% Neu5A. Scale bars indicate 10 mm.

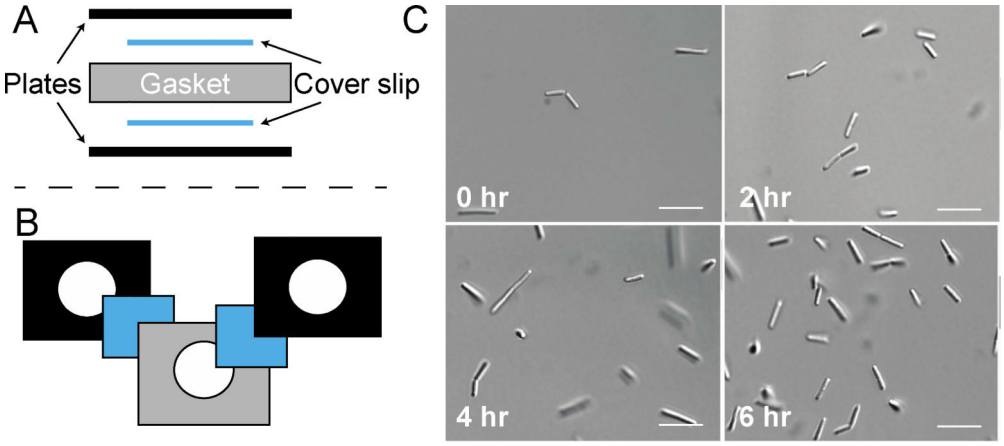

Figure 2. Extended live-cell microscopy of *C. difficile* R20291.

(A) Side view of rose chamber assembly. Aluminum top and bottom plates (black) are screwed together to hold the chamber together. A gas impermeable gasket (grey) is used to contain the sample between two cover slips (blue) and to prevent oxygen poisoning of the sample. (B) Top view of rose chamber assembly. (C) Growth of *Clostridioides difficile* R20291 within the imaging chamber in BHIS medium. Growth and motility of bacteria were observed while sealed in the imaging chamber and kept at 37 °C. Panels show time course of 0, 2, 4, and 6 hours as indicated. Scale bar indicates 10 μm.

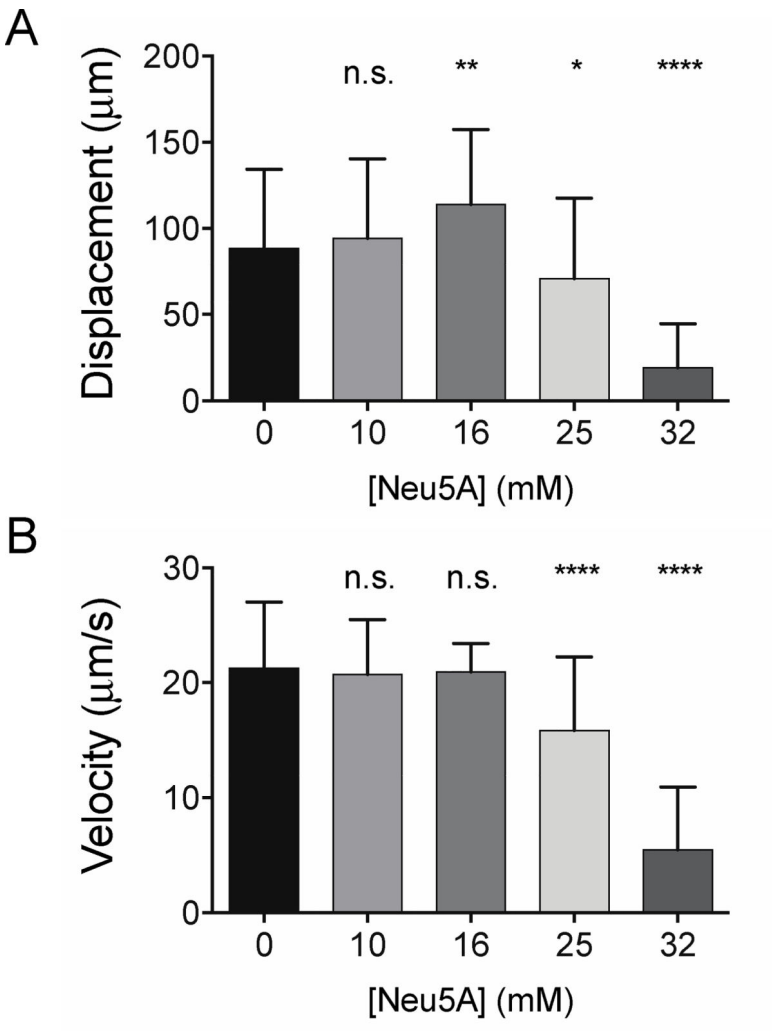

Figure 3. Nutrient supplementation reduces net displacement and linear run velocity.

(A) Net cell displacement of *C. difficile* R20291 within 10 seconds in BHIS containing the indicated concentration of Neu5A. (B) Linear swimming velocity during unidirectional runs in BHIS-agar containing the indicated concentration of Neu5A. Shown are the means and standard deviations of 49–146 cells per condition. Displacement and velocity of cells in supplemented media were compared to those in unsupplemented BHIS by one-way analysis of variance using Tukey's multiple comparison test. n.s. not significant; **** $p < 0.0001$.

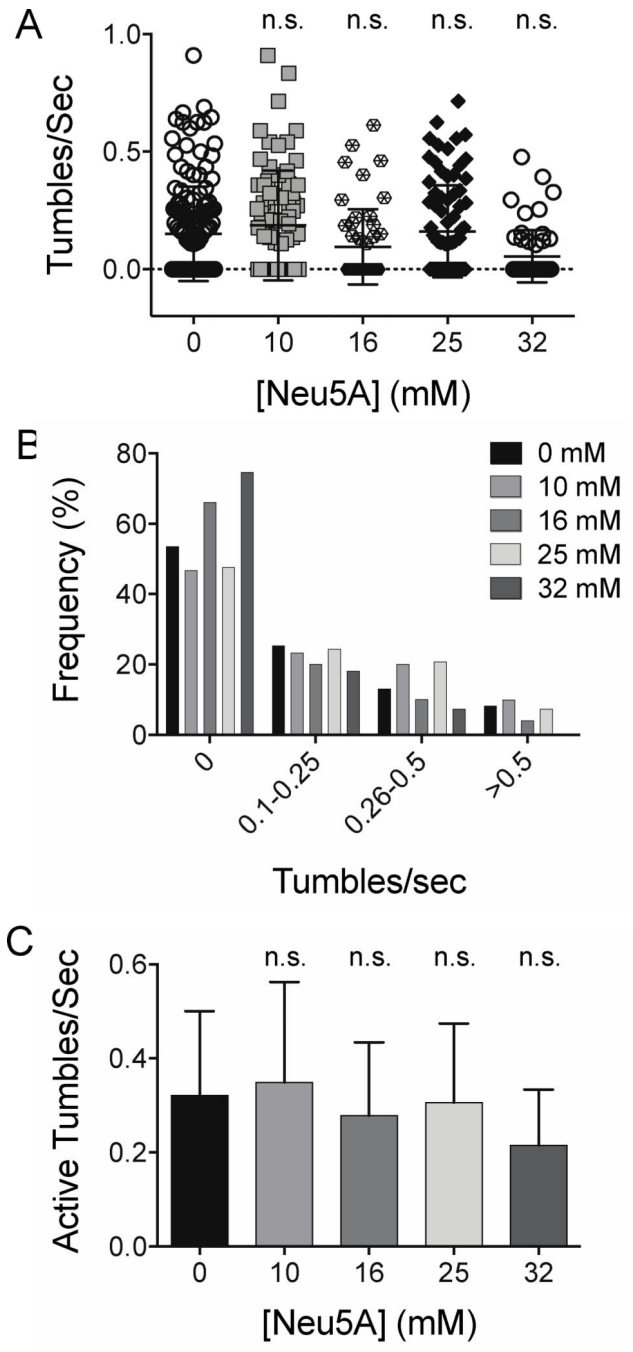

Figure 4. Nutrient effect on *C. difficile* R20291 tumbling.

(A) Tumble frequency of *C. difficile* R20291 in BHIS supplemented with the indicated concentration of Neu5A. Tumble counts were normalized by the duration of each individual cell's motility to control for cells that swam out of the field of view during the 10 second counting interval. (B) Percentage of the total cells exhibiting the indicated number of tumbles/second in each condition. (C) Normalized tumbling frequency of the cells that exhibited a non-zero rate of tumbling. Shown are the means and standard deviations of 49–146 cells per condition. Tumble frequencies of all cells and of tumbling cells in each

medium condition were compared to those in unsupplemented BHIS by one way analysis of variance using Tukey's multiple comparison test. n.s. not significant.

Table 1.

Doubling times of *C. difficile* R20291 in BHIS with 1% supplementation.

Medium	Doubling time (hr)
BHIS	1.74
BHIS-1% arabinose	1.54
BHIS-1% glucose	1.59
BHIS-1% Neu5A	1.30

Doubling times were calculated between 0 and 5 hours of growth in the indicated media.